R-99-38

Subglacial groundwater flow at Äspö as governed by basal melting and ice tunnels

Urban Svensson
Computer-aided Fluid Engineering AB

February 1999

Svensk Kärnbränslehantering AB
Swedish Nuclear Fuel
and Waste Management Co
Box 5864
SE-102 40 Stockholm Sweden
Tel 08-459 84 00
+46 8 459 84 00
Fax 08-661 57 19
+46 8 661 57 19

SKB

ISSN 1402-3091
SKB Rapport R-99-38

Subglacial groundwater flow at Äspö as governed by basal melting and ice tunnels

Urban Svensson

Computer-aided Fluid Engineering AB

February 1999

ABSTRACT

A high resolution three dimensional numerical model of subglacial groundwater flow is described. The model uses conductivity data from the Äspö region and is thus site specific. It is assumed that the groundwater flow is governed by the basal melting and ice tunnels; ice surface melting is not considered.

Results are presented for the meltwater transport time (to the ice margin) and maximum penetration depth. Conditions at repository depth, i.e. about 500 metres, are also analysed.

The general conclusion from the study is that the model presented gives plausible results, considering the basic conceptual assumptions made. It is however questioned if the hydraulics of the ice tunnels is well enough understood; this is a topic that is suggested for further studies.

TABLE OF CONTENTS

1 INTRODUCTION

It is anticipated that spent nuclear fuel will be stored in deep repositories. Even if a repository is located in a crystalline rock of low permeability a leak from the repository may find its way to the biosphere. The transport takes place in the fracture system in the rock. Future climate changes may change both the fracture system and the flow within it and it is thus important to assess the magnitude and effects of this expected future impact on a repository.

In this report the subglacial groundwater flow due to basal melting will be studied. The study is site-specific as the conductivity field (including effects of fracture zones) is generated from data for the Äspö area. Traces of the inland ice can be found in the area in form of eskers. In the numerical model ice tunnels will be placed where these eskers are found. It is one of the key issues in the study to evaluate the effect of ice tunnels. Other aspects of the problem that will be focused upon include meltwater penetration depth and transport times from expected repository depth, i.e. about 500 metres.

2 BASIC CONCEPTUAL ASSUMPTIONS

The study attempts to simulate the conditions at Äspö at the time of the retreat of the last inland ice, i.e. about 11 000 years BP (before present). The ice margin will be placed right on Äspö with an orientation as given in Figure 2-1. In the Äspö region eskers have been found with a spacing of about 10 km. In Figure 2-1 the two thick lines indicate esker locations. It is assumed that ice tunnels were formed in the glacier, where the eskers are found today. In the numerical model to be described, the lateral boundaries (roughly east and west boundaries) will be placed along the eskers. It is thus assumed that the ice tunnels generate symmetry lines in the flow, pressure and salinity distributions. In the south-north direction, i.e. along the ice movement, the computational domain needs to be of the order 250 km in order to describe the flow and salinity distribution under the ice-front (Svensson 1996).

After this general introduction to the problem formulation we will, guided by Boulton et al (1995), list the basic assumptions of the simulation model:

- The simulation is quasi-steady. All boundary conditions are in a steady state and the ice margin will be over Äspö for the whole period simulated, which is 1 000 years.

- The computational domain is three-dimensional with dimensions 250 x 10 x 4 km^3 (Length x Width x Depth), see Figure 2-2.

- No heat flux is considered.

- The ice-front is assumed to have a shape governed by a sine curve, with a length of 100 km and a maximum height of 1 km.

- The meting rate is also assumed to be distributed according to a sine curve, with a maximum melting rate of 50 mm/year.

- The ice tunnels are simulated as strings of cells with a higher conductivity than the ambient ground.

- Initial salinity distribution is given as zero salinity down to 1 000 metres, below this level a linear increase with 10% per 1 000 metres is prescribed.

- The kinematic porosity will be given the value 10^{-3}.

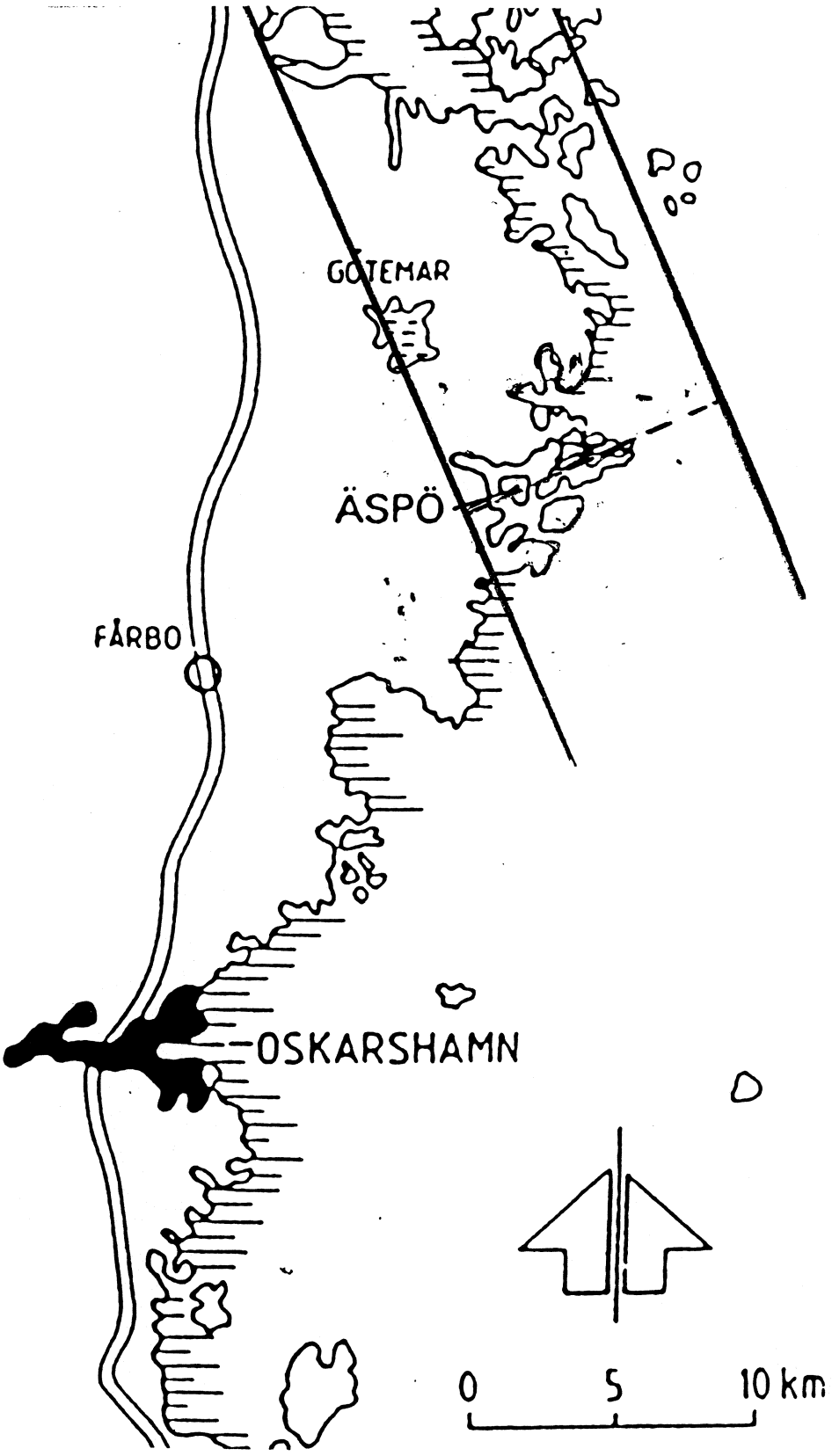

Figure 2-1. *The Äspö region. The two thick lines mark eskers and the broken line shows the assumed position of the ice margin.*

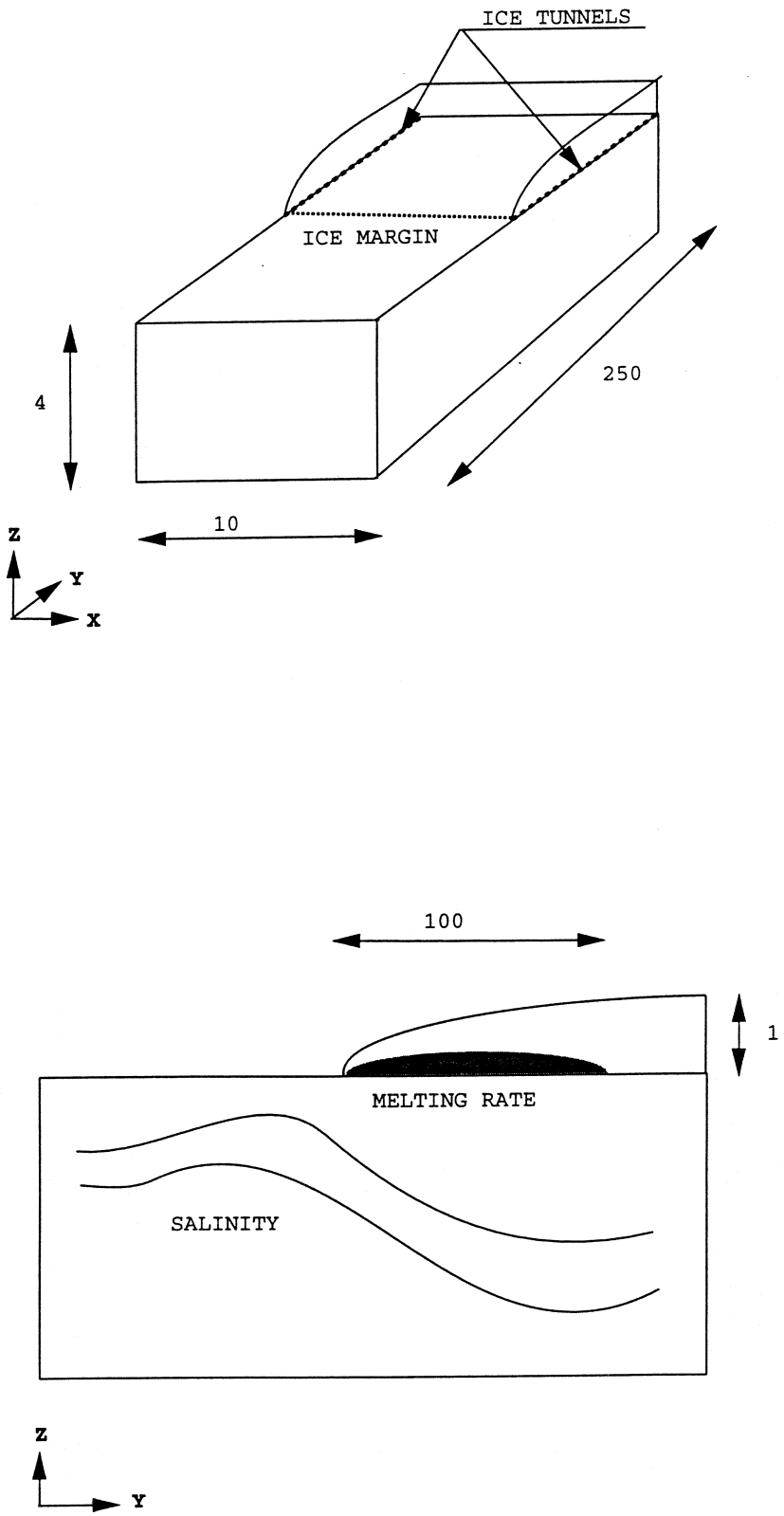

Figure 2-2. *Computational domain. Perspective view (top) and vertical section. All distances in km.*

These are the main assumptions of the model; further details about conductivity fields, boundary conditions, etc will be given in the next section.

In the calibration of the model a basic conceptual idea is used. As the meltrate is fixed a certain pressure below the ice will result. Obviously this pressure can not be larger than the ice load, as the ice would then float (and create the space needed for the drainage). In the calibration, the conductivity of the "ice tunnel cells" will be given a value which generates a subglacial pressure which is everywhere smaller than the pressure from the ice load.

3 MATHEMATICAL MODEL

3.1 BASIC APPROACH AND ASSUMPTIONS

The main conceptual assumptions were introduced in the previous section. For the mathematical/numerical model the following can be added:

- For the momentum balance it is assumed that the Darcy law applies.
- Variable density needs to be accounted for, as the salinity of the groundwater will vary in the computational domain.
- The computational domain was introduced in Figure 2-2. This domain will be discretized with a computational grid of 587 500 cells (50 x 250 x 47) (Width x Length x Depth). The grid is cartesian with nonuniform spacing; details below.

3.2 GOVERNING EQUATIONS

Within the assumptions, the following set of equations can be formulated.

Momentum:

$$0 = -\frac{\partial p}{\partial x} - \frac{\rho g}{K_x} u \tag{1}$$

$$0 = -\frac{\partial p}{\partial y} - \frac{\rho g}{K_y} v \tag{2}$$

$$0 = -\frac{\partial p}{\partial z} - \frac{\rho g}{K_z} w - \rho g \tag{3}$$

Salinity balance:

$$n\frac{\partial s}{\partial t} + \frac{\partial}{\partial x}us + \frac{\partial}{\partial y}vs + \frac{\partial}{\partial z}ws = \frac{\partial}{\partial x}\left(D\frac{\partial s}{\partial x}\right) + \frac{\partial}{\partial y}\left(D\frac{\partial s}{\partial y}\right) + \frac{\partial}{\partial z}\left(D\frac{\partial s}{\partial z}\right) \tag{4}$$

Mass balance:

$$\frac{\partial}{\partial x}\rho u + \frac{\partial}{\partial y}\rho v + \frac{\partial}{\partial z}\rho w = 0 \qquad (5)$$

Equation of state:

$$\rho = \rho_0(1 + \alpha s) \qquad (6)$$

Where *u, v, w* are Darcy velocities, *p* pressure, *s* salinity (in %, by weight), K_x, K_y, K_z conductivities, *D* hydraulic dispersion coefficient, *n* kinematic porosity $(= 10^{-3})$, α a coefficient $(= 7.41 \times 10^{-3})$, ρ_0 a reference density of water (= 1 000 kg/m^3), ρ density of water and g gravitational acceleration. The coordinate system is denoted *x, y, z* with *x* in the east direction, *y* north and *z* vertical upwards.

It is still unclear (at least to the author) how the hydraulic dispersion coefficient ought to be interpreted and determined in a fractured rock. For a general porous media, where a representative elementary volume can be defined, general tensor expressions are available, see Bear et al (1987). A further complicating factor is that we are going to apply the salinity equation in a discretized form, i.e. on our computational grid. A suggestion is that the dispersion coefficient should account for sub-grid mixing processes. Due to the uncertainty about the interpretation of the process we will assume that the dispersion coefficient is isotropic, proportional to the local velocity and the grid-size, hence:

$$D = \beta \Delta |\vec{U}| \qquad (7)$$

where β is an unknown coefficient, Δ the grid-spacing and $|\vec{U}|$ the magnitude of the Darcy-velocity. As seen, the effect of molecular diffusion is also neglected in (7). A constant value of 5 metres was set for the product $\beta\Delta$.

3.3 GEOMETRIC FRAMEWORK AND MATERIAL PROPERTIES

The major transmissive fracture zones in the region are shown in Figure 3-1. The transmissivities have been estimated, see Rhén et al (1997), to be 10.0×10^{-5} m^2/s. In Rhén et al fractures with a transmissivity of 1.0×10^{-5} m^2/s are also given. These are not included in this study, as they would contribute insignificantly to the conductivity field on the scale studied. In fact, also the fractures included give a very small contribution to the conductivity fields.

Hydraulic conductivities at different depths for the rock in between the fracture zones have been estimated from field measurements, see Rhén et al (1997). It is well-known that these conductivities, and their standard deviations, vary with the test scale. When a numerical model is set-up one needs to consider the relation between the cell size in the grid and the test scale. The values given in Table 3-1 represent a test scale of 100 metres, except for the values for depth > 600 metres, which are for a test scale of about 300 metres. The computational grid has a non uniform grid spacing with increasing cell size with depth and with distance from ice margin (details below). At the ice margin the horizontal grid spacing is 200 metres and below a depth of 200 metres the vertical grid size is uniform with $\Delta_z = 100$ metres. As it is not obvious how to scale the conductivities for a non uniform grid with large aspect ratios $(\Delta_y / \Delta_x >> 1)$, the values in Table 3-1 were used as given by Rhén et al (1997).

Table 3-1. Rockmass hydraulic conductivity and its standard deviation for the region considered. After Rhén et al (1997).

Depth (m)	K (m/s)	s ($\log_{10}$ K)
0 - 200	1.3 E-7	0.96
200 - 400	2.0 E-7	0.65
400 - 600	2.6 E-7	0.79
600 →	4.7 E-8	0.72

The computational grid is shown in Figure 3-2. In the x-direction a uniform cellsize of 200 metres is used. In the vertical direction the grid expands from ground level downwards. The following sequence of Δ_z is used: 5 x 10, 20, 30, 40 and 60 metres. This adds up to 200 metres; below this depth Δ_z is 100 metres down to 4 000 metres . In the y-direction Δ is 200 metres at the ice margin and expands in the north and south directions. The total numbers of grid cells is 587 500 (50 x 250 x 47).

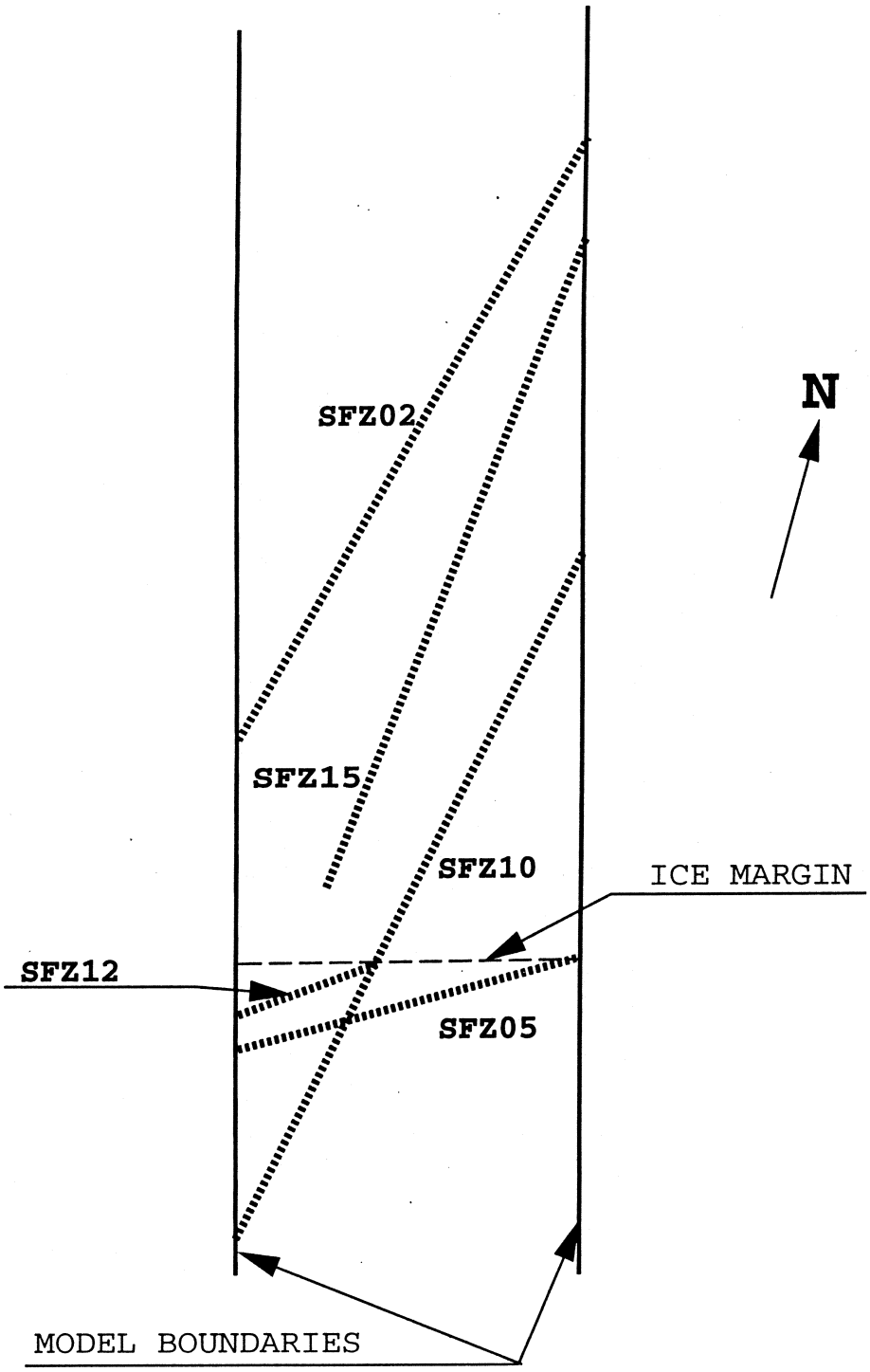

Figure 3-1. *Major fracture zones in the area, after Rhén et al (1997).*

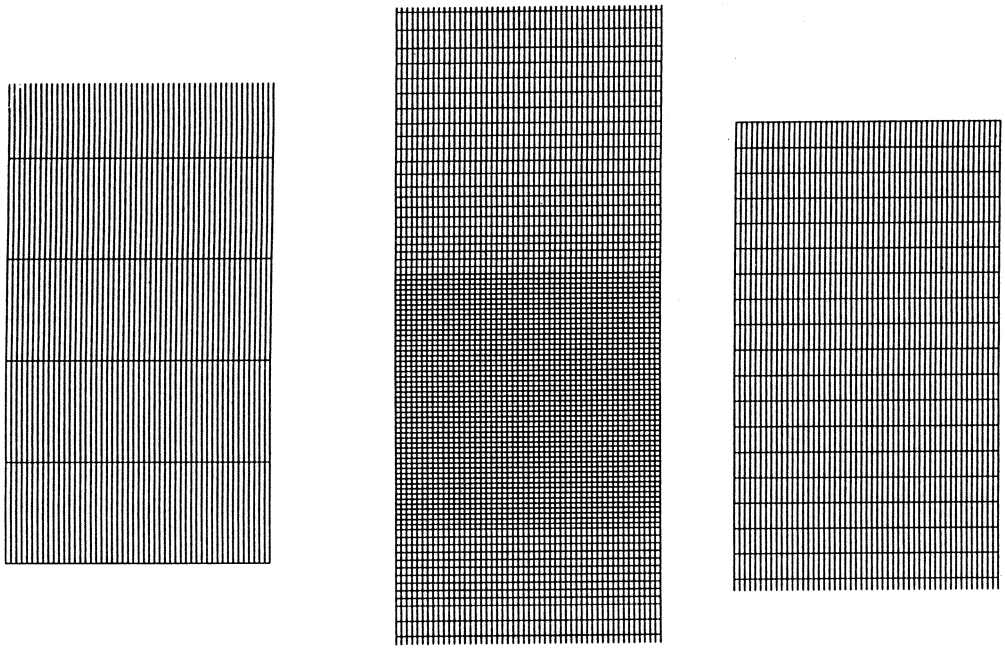

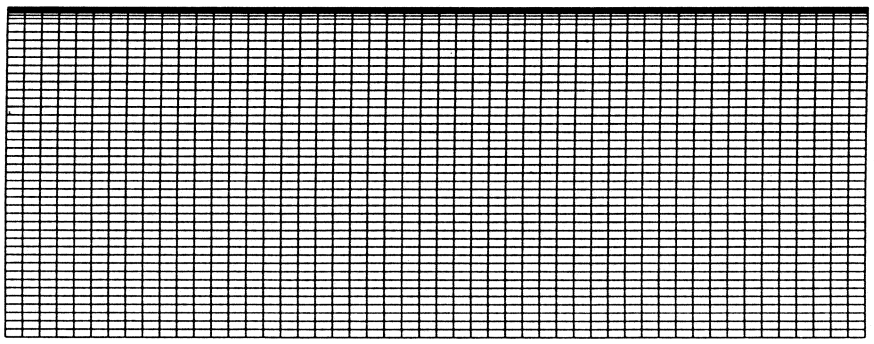

Figure 3-2. *Computational grid. Horizontal sections (top) and a vertical section.*

3.4 SPATIAL ASSIGNMENT METHOD

The conductivity and transmissivity data given in the previous section need to be assigned to the computational grid. The main steps in this procedure are:

- Generate a conductivity randomly for each computational cell using the geometric mean values and standard deviations given in Table 3-1. No correlation is assumed between the cells.

- Generate cell wall conductivities by calculating a geometric mean between the cell and its neighbour. This is done for all cell walls and hence gives a locally anisotropic conductivity, i.e. for a given cell all cell wall conductivities are different.

- Calculate the length of the fracture zone crossings for each cell wall. Modify the cell wall conductivity with respect to the transmissivity of the fracture zones.

Further details about the third point can be found in Svensson (1997).

3.5 BOUNDARY CONDITIONS

At the top boundary the meltwater flux is prescribed below the ice, with a salinity of 0%. South of the ice margin a zero pressure condition is used.

At the vertical and bottom boundaries zero flux conditions are used for all variables

3.6 NUMERICAL TOOL AND OUTPUT PARAMETERS

The system of equations is solved by the general equation solver PHOENICS, Spalding (1981). PHOENICS is based on a finite-volume formulation of the basic equations and embodies a wide range of coordinate systems (cartesian, body-fitted, cylindrical, etc) and numerical techniques (higher order schemes, solvers, etc).

The basic output parameters from the model are pressure, salinity and Darcy velocities. It is however simple to generate additional output parameters like hydraulic head and density.

4 RESULTS

4.1 INTRODUCTION

In the presentations of results a reference situation will first be discussed. This situation follows the problem specification outlined in section 2. After that the sensitivity to the initial salinity distribution and the conductivity of the ice tunnels will be analysed. The final section deals with conditions at repository depth.

4.2 THE REFERENCE CASE

As mentioned, the specification of this case has already been given. The conductivity of the ice tunnel cells was however left as a calibration parameter, with the condition that the conductivity should generate a subglacial pressure which is everywhere smaller than the pressure from the ice load. A conductivity of 0.02 m/s is found to fulfil this condition, as can be seen in the ground level fresh water head distribution shown in Figure 4-1. In the region with maximum head the ice thickness is about 800 metres and the ice pressure, with $\rho_{ice} = 900$ kg/m^3, is thus somewhat larger than the pressure due to basal melting.

The Darcy flow distributions in two sections are shown in Figure 4-2 and 4-3. In the horizontal section, Figure 4-2, it can be seen that most of the meltwater will be discharged through the ice tunnels. In the vertical section one may note that the vectors are smaller below a depth of 600 metres; this is due to the conductivity distribution as given in Table 3-1. The salinity distributions in two vertical sections are shown in Figure 4-4. As can be seen there is an upconing effect below the ice tunnels. At the ice margin the salt water will reach ground level, which means that the total salt content in the domain is decreasing.

One of the key questions in this work is to analyse the destiny of the basal meltwater. For this purpose a string of particles are placed at ground level from the ice margin to a point 100 km north of it; all at a mid-position in the x-direction. First 200 particles were released along this line each year and tracked for 100 years. The result can be studied in Figure 4-5. As expected most of the particle tracks will end up in the ice tunnels. Next 500 particles were released along the same line and these were tracked for 600 years. This was done with the purpose to estimate travel times (to ice margin) and penetration depths. The result can be studied in

Figure 4-6. It is found that most of the particles will have a travel time of less than 100 years and typically reach a depth of 2 000 metres. For the particle tracking simulations it is assumed that the kinematic porosity, n_e, is related to the conductivity, K, in the following way, see Rhén et al (1997):

$$n_e = 34.87K^{0.753}$$

with the constraint that $n_e \leq 0.05$.

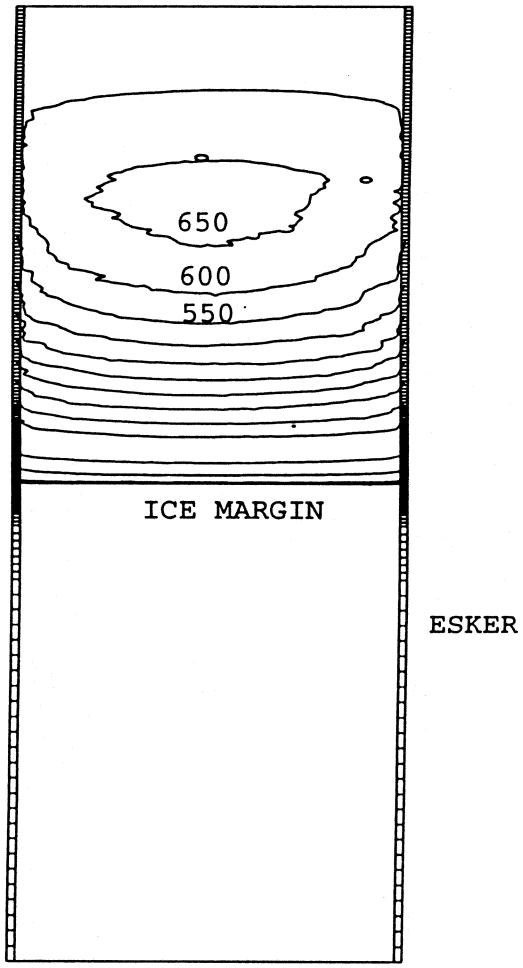

Figure 4-1. *Freshwater head at ground level.*

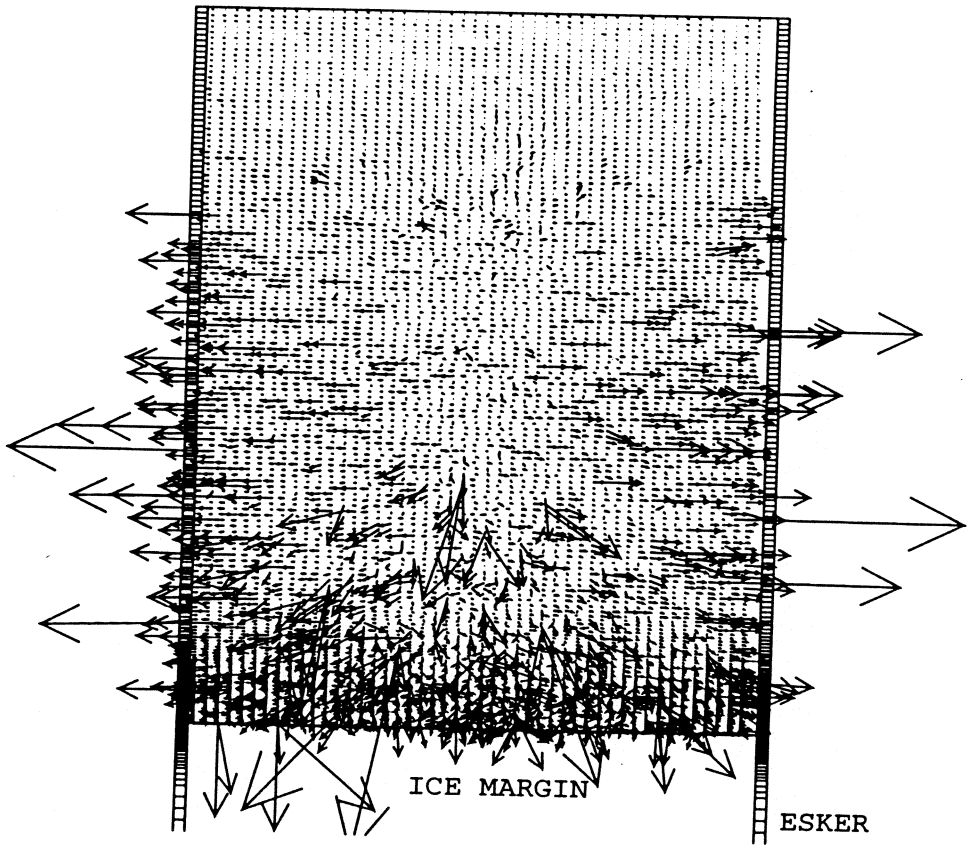

Figure 4-2. *Darcy flow vectors at ground level.*
Velocity scale: ⟶ 10^{-7} *m/s.*

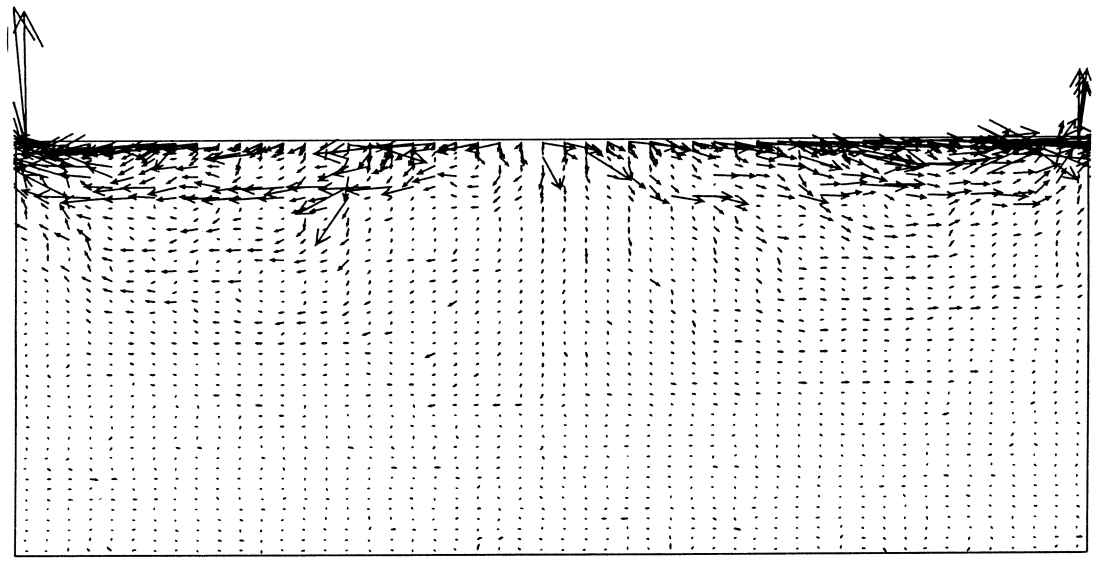

Figure 4-3. *Darcy flow vectors in a vertical section 1 km from the ice margin. Velocity scale:* ⟶ 2×10^{-8} *m/s.*

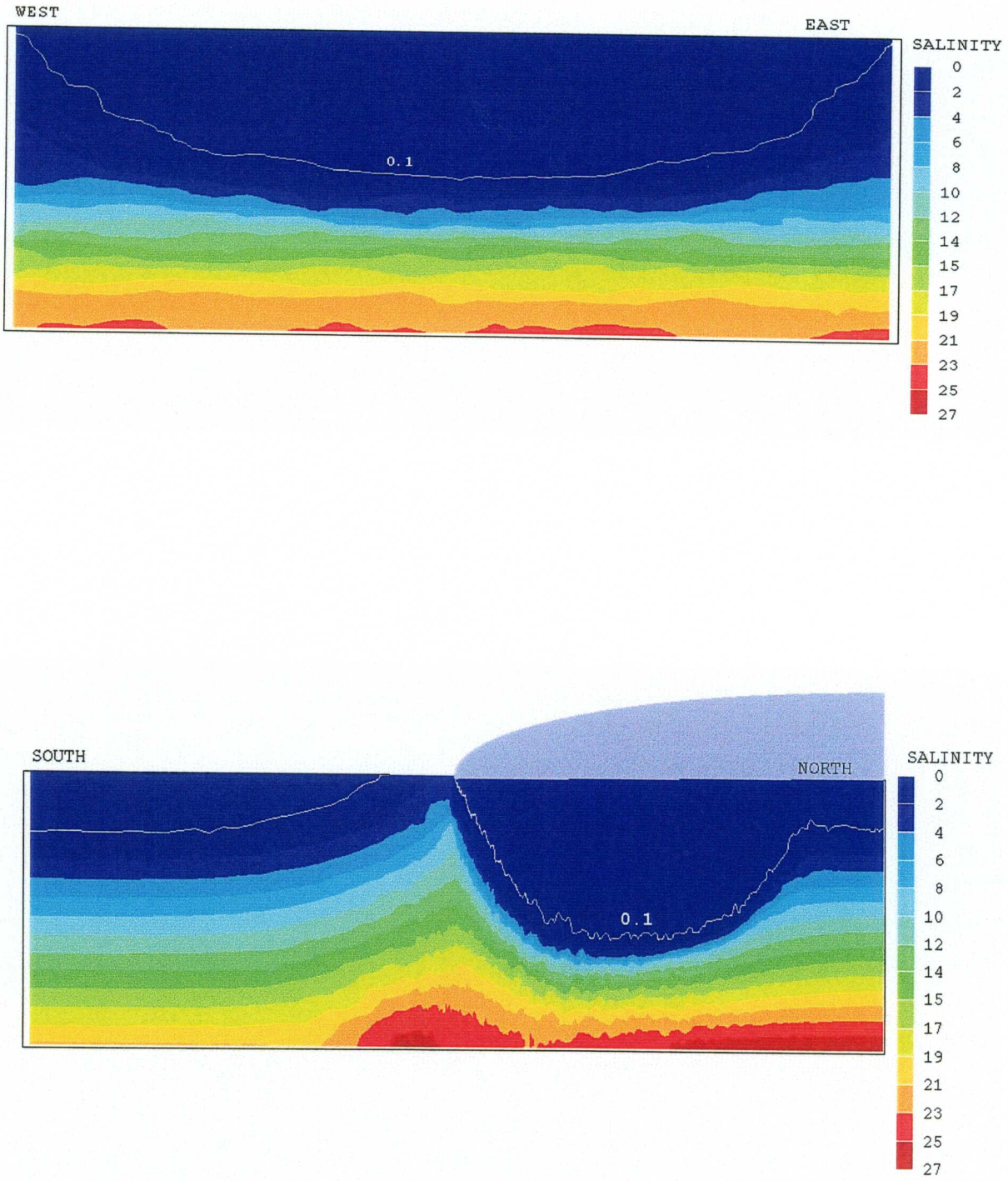

Figure 4-4. *Salinity distributions in two vertical sections.*
The east-west section is located 25 km from the ice margin and the north-south section in the middle of the domain.

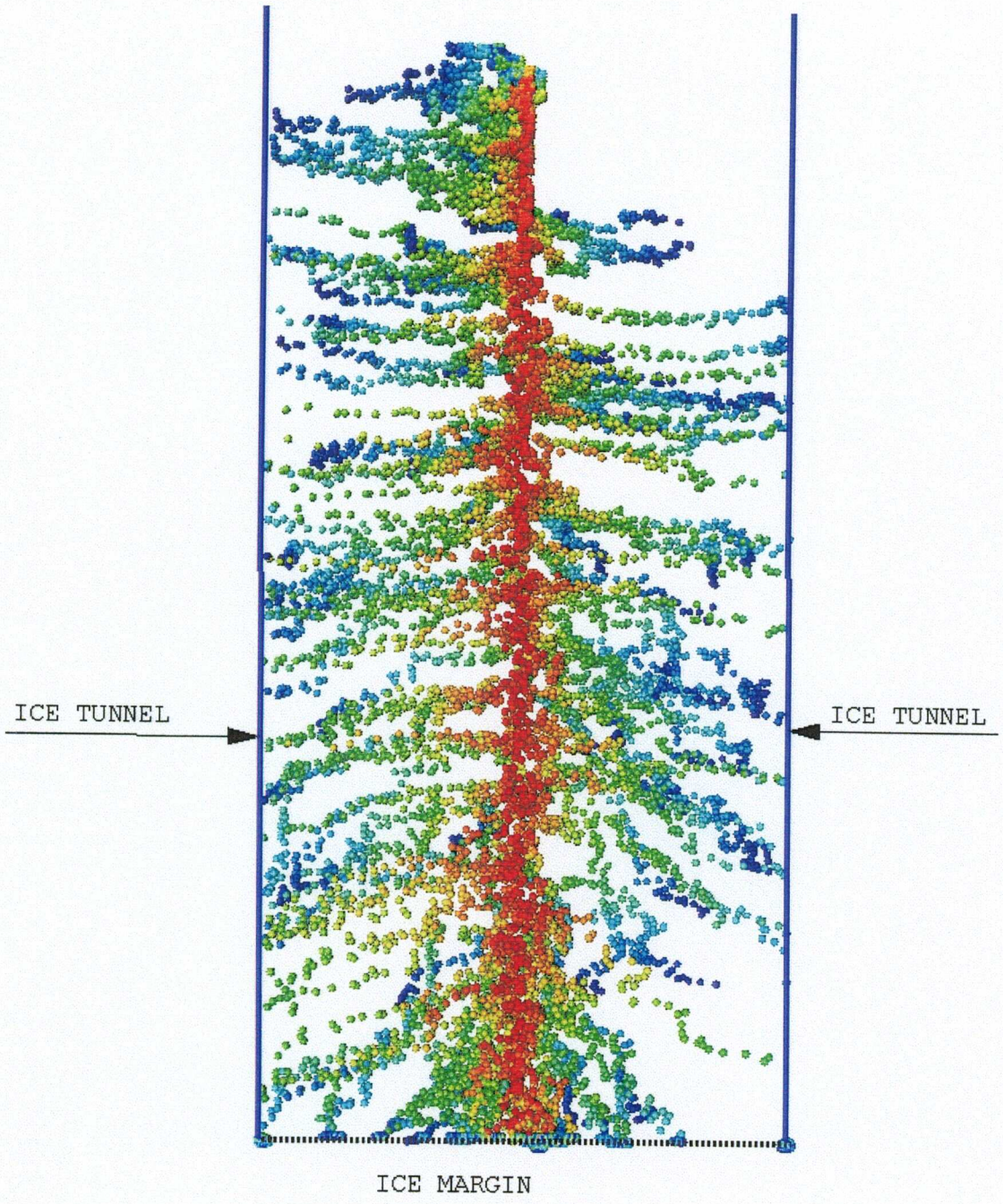

Figure 4-5. *Flow paths for basal meltwater. 200 particles were released each year under 100 years along a south-north line. Red particles have been released recently, while dark blue particles were released 100 years earlier.*

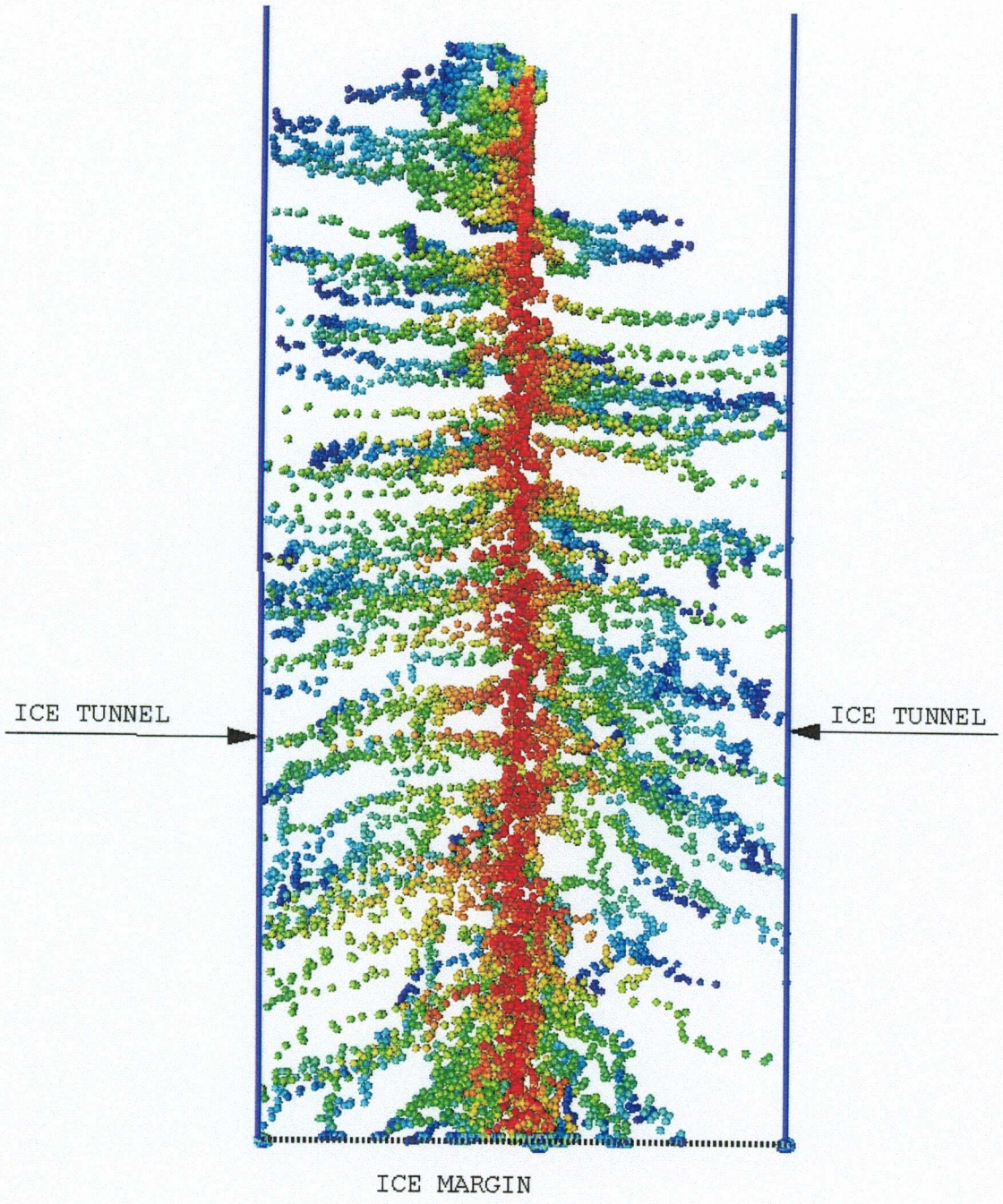

Figure 4-5. *Flow paths for basal meltwater. 200 particles were released each year under 100 years along a south-north line. Red particles have been released recently, while dark blue particles were released 100 years earlier.*

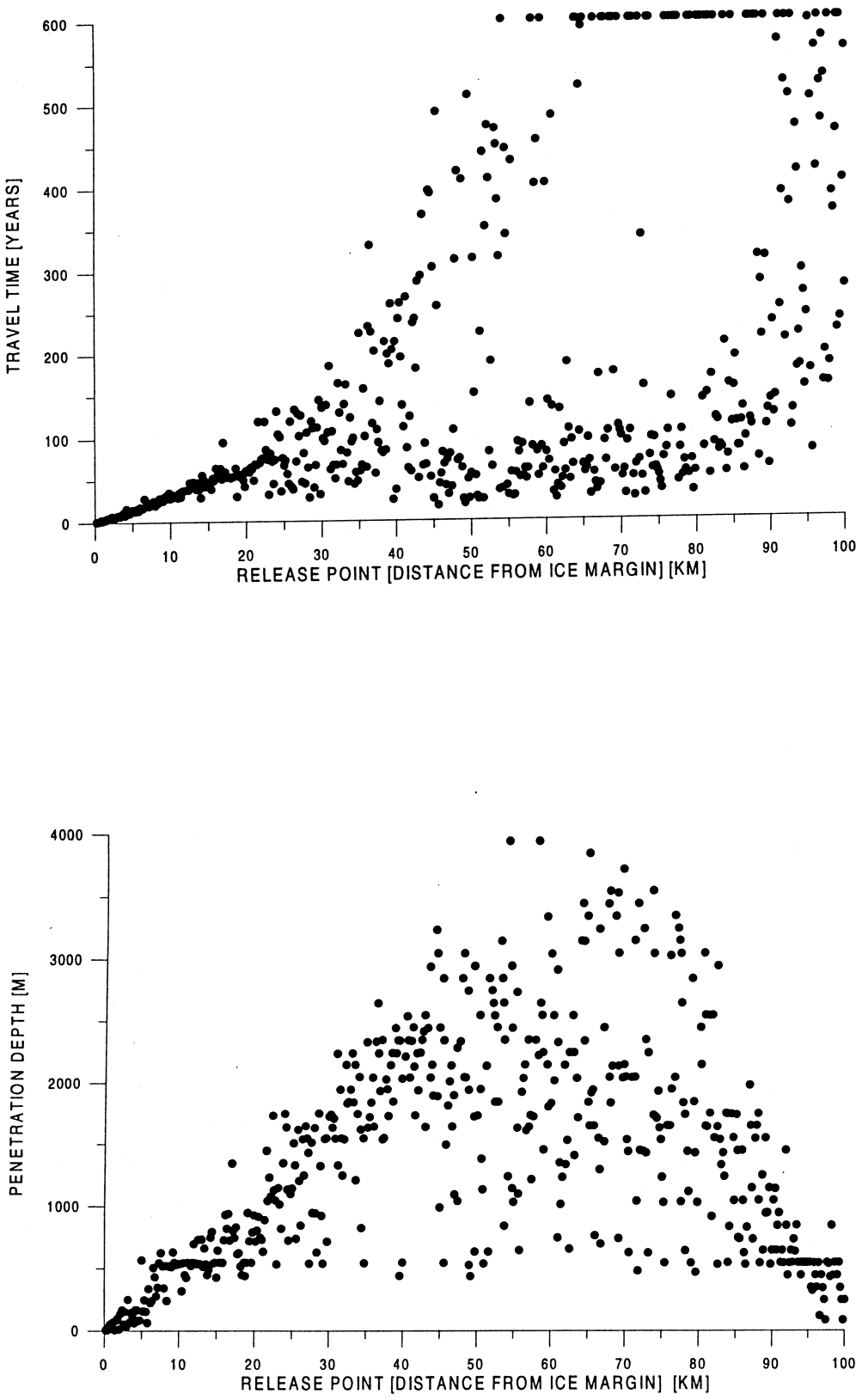

Figure 4-6. *Travel time to ice margin (top) and maximum penetration depth for 500 particles released along a south-north line in the centre of the domain.*

4.3 SENSITIVITY STUDIES

In section 2 the initial salinity distribution was specified as zero down 1 000 metres and thereafter an increase with 10% per 1 000 metres. The first sensitivity study concerns this initial salinity profile. The alternative salinity profile is zero down to 600 metres and thereafter increases with 10% per 1 000 metres. One reason for picking the depth 600 metres is that the conductivity is significantly lower below this depth, see Table 3-1. The main result of this test was that the alternative initial salinity profile did not change the results significantly after 1 000 years of integration. There is thus no point in repeating all the figures from the reference case; only Figure 4-7 is shown to demonstrate the result. As can be seen in this figure the meltwater penetration depth is very similar for the two cases.

The next sensitivity study to be discussed concerns the conductivity of the ice tunnels. In the reference case a conductivity of 0.02 m/s was found to give a subglacial pressure which is everywhere smaller than the pressure from the ice load. What will happen if the conductivity is an order of magnitude larger, i.e. 0.2 m/s? The results of such a simulation can be studied in Figures 4-8 and 4-9. From Figure 4-8 it is clear that the pressure and flow distributions are very sensitive to this change; the maximum pressure is now only 25% of the value in the reference case. Also the travel time and penetration depth of meltwater are modified. The average penetration depth is reduced with about 500 metres.

4.4 IMPACT ON A REPOSITORY

We will now return to the reference conditions and study the implications for a repository at a depth of 500 metres. Conditions along the south to north line used earlier (but now at a depth of 500 metres) will be discussed. The reason for studying the conditions along a line is that a repository will experience all conditions along this line due to the ice movement.

In Figure 4-10 particle tracks from 500 metres depth can be studied. Two hundred particles were released every year during one hundred years. The particles have been coloured with respect to time since release; red ones are newly released while dark blue ones were released hundred years earlier. Considering that the length of the "release line" is 100 km, one would perhaps expect more pathways to the ice tunnels. A detailed picture of the travel time distribution is given in Figure 4-11, where also the Darcy velocity magnitude at repository depth is shown. Close to the ice margin the travel time to ground level is very short, while a typical travel time of 100 years is found further away from the ice margin. The median travel time is 108 years and the median $\log_{10}$ (velocity magnitude) is -8.6 m/s.

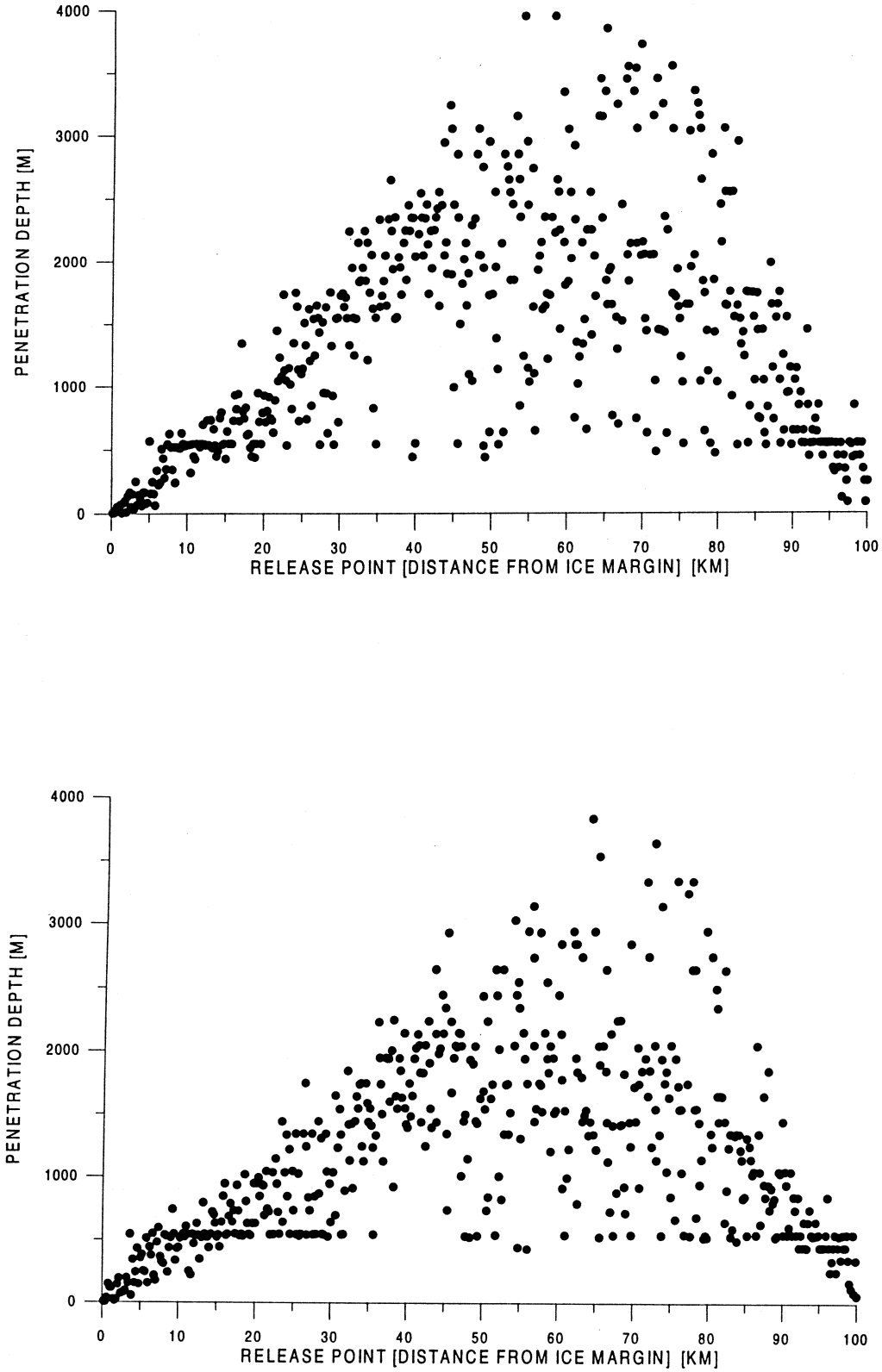

Figure 4-7. *Penetration depth for meltwater. Sensitivity to initial salinity profile. Reference case (top) and salinity profile that increases from a depth of 600 metres.*

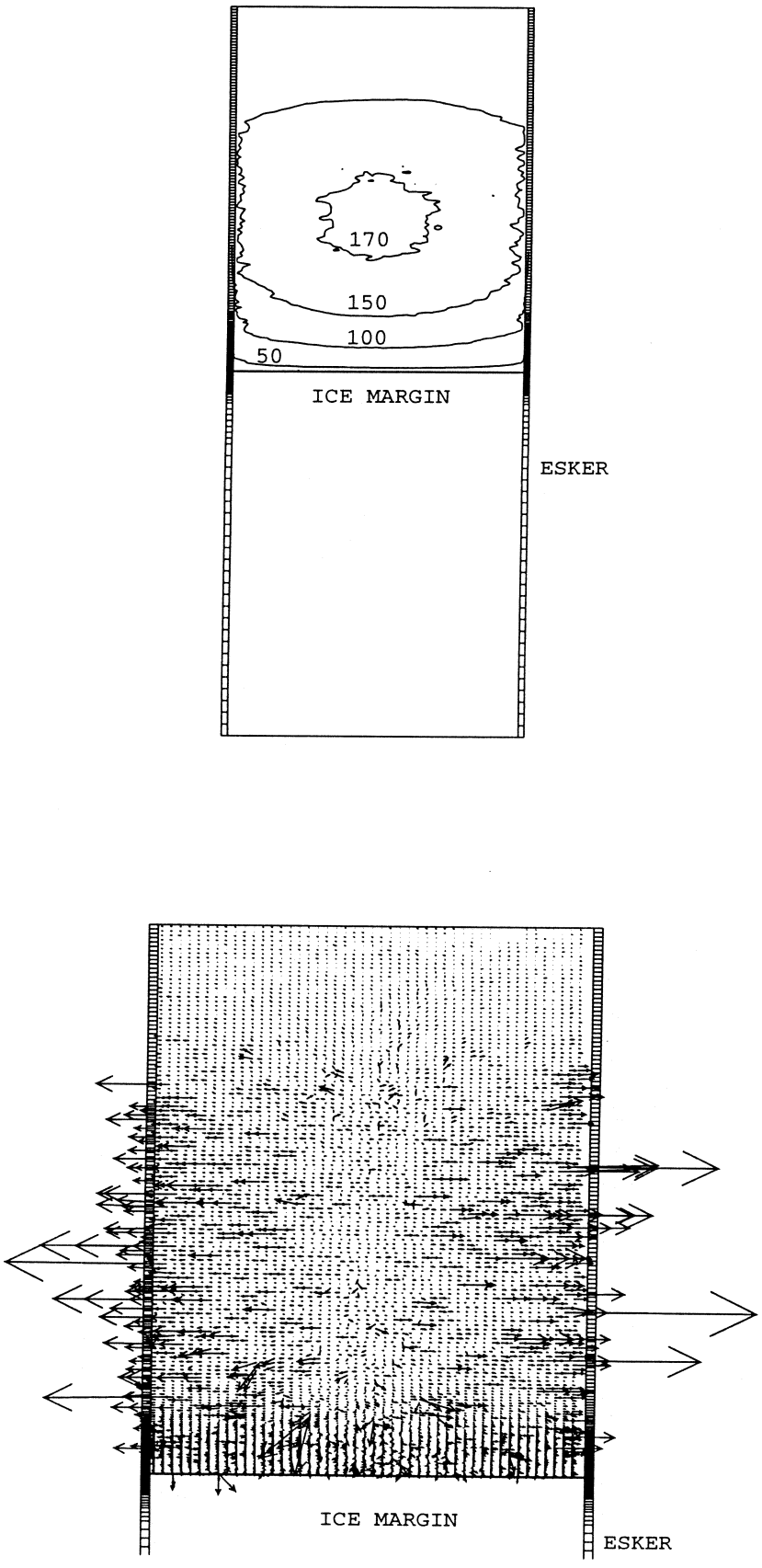

Figure 4-8. *Freshwater head (top) and Darcy flow vectors at ground level for an ice tunnel conductivity of 0.2 m/s. Velocity scale:* ⟶ 10^{-7} *m/s.*

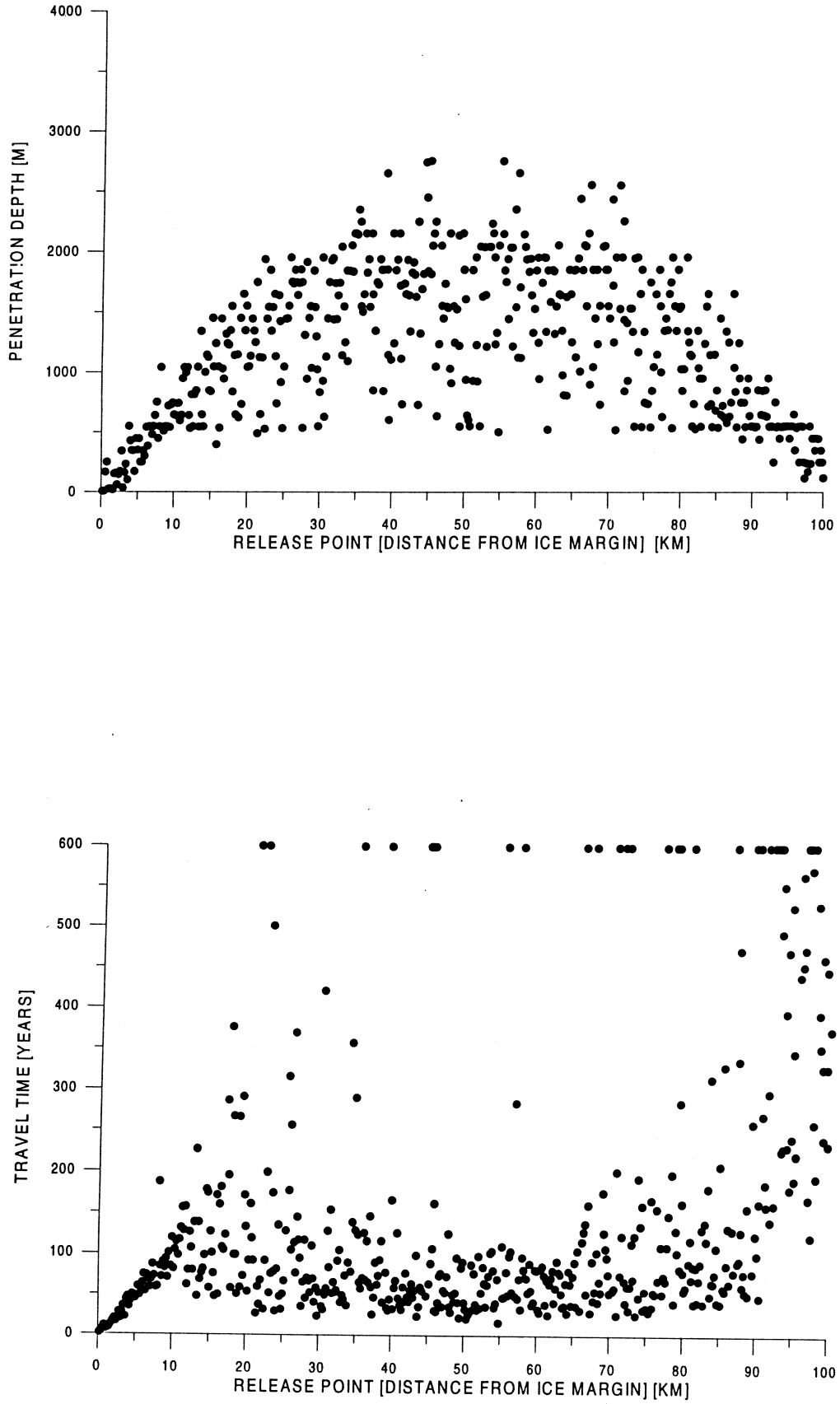

Figure 4-9. *Meltwater penetration depth (top) and travel time for an ice tunnel conductivity of 0.2 m/s.*

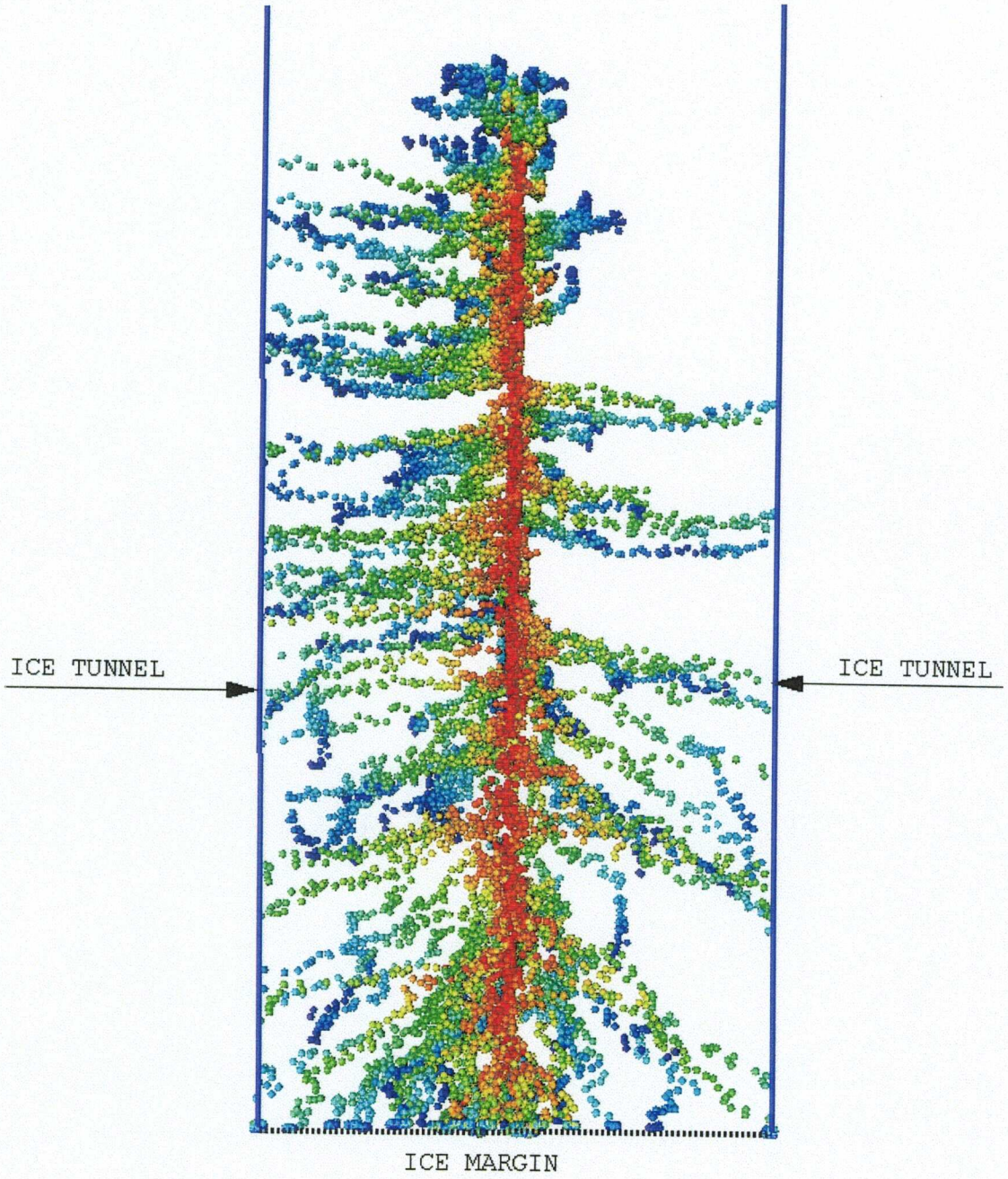

Figure 4-10. *Flow paths from repository level, 200 particles were released each year under 100 years, along a south-north line. Red particles have been released recently, while dark blue ones were released 100 years earlier.*

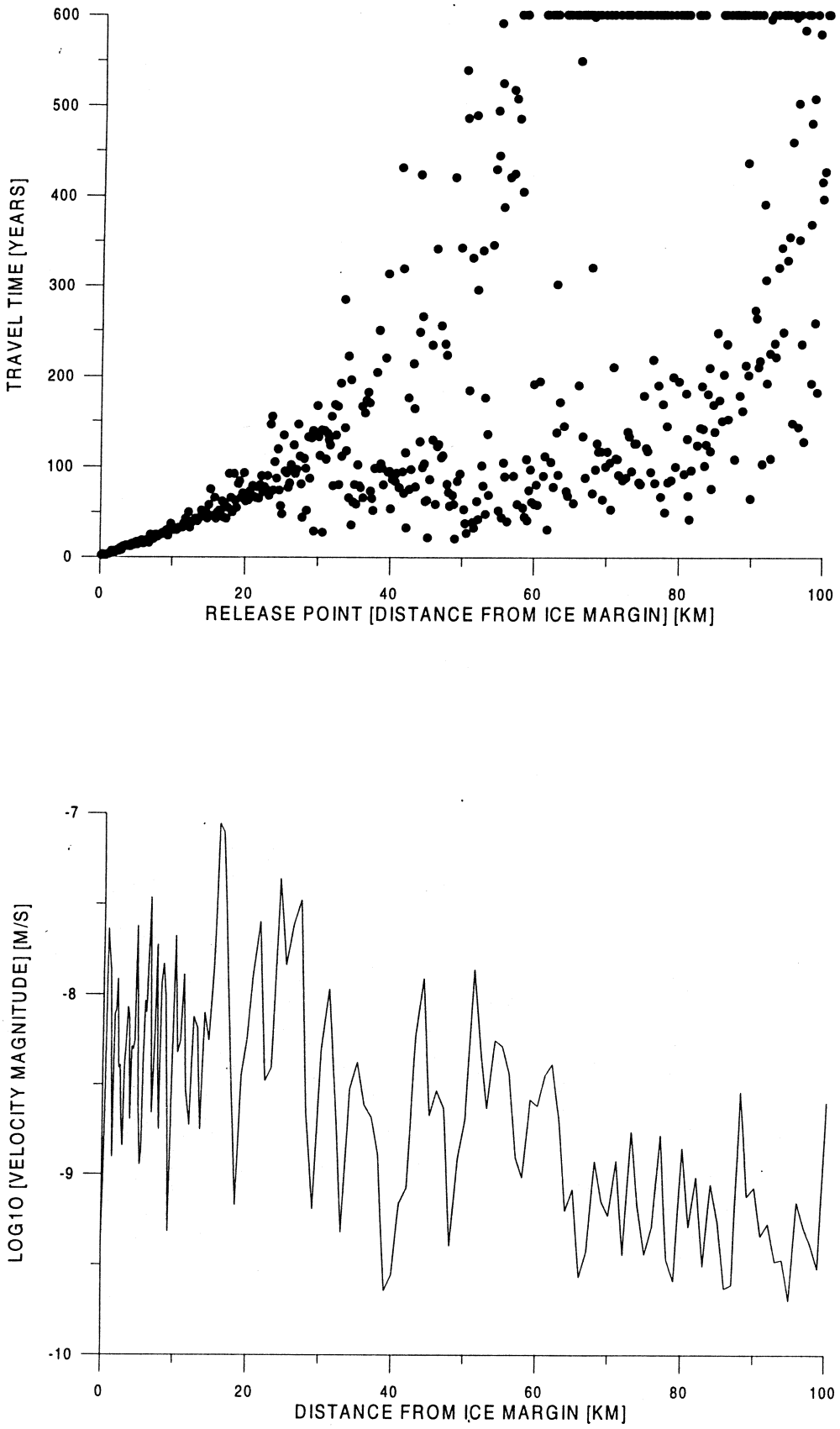

Figure 4-11. *Travel times from repository level to ground (top) and Darcy velocity magnitude at repository level.*

5 DISCUSSION AND CONCLUSIONS

It is now time to evaluate the relevance and significance of the simulations presented. One thing that has been demonstrated is that high resolution numerical simulations of subglacial groundwater flow can be performed. Another question is how relevant these are. This question relates back to the basic conceptual assumptions made. Guided by the sensitivity studies presented, it seems that the assumptions regarding the ice tunnels are the most crucial ones. In order to improve the relevance and significance of the simulations it is therefore suggested that the following aspects of the problem need to be studied in more detail:

- The hydraulics of the ice tunnels, i.e. flow, pressure distributions, transient effects, secondary channel systems, length, spacing, etc.

- Related to this is the transport of ice surface meltwater. This meltwater can probably by an order of magnitude larger than the basal meltwater considered in this report. As the surface meltwater will affect the pressure distribution in the ice tunnels one may need to consider it in the simulations.

There are of course a number of additional topics that are relevant to study (for example, will the ice load modify the hydraulic conductivity of the rock?) but it is the author's view that the assumptions regarding the ice tunnels are the most crucial ones in a simulation of the kind presented.

In light of the simulations presented and the above discussion one has to be rather cautious with conclusions. What has been clearly demonstrated is that site-specific simulations of subglacial groundwater flow can be performed technically. The model presented is based on the relevant conservation equations and produces results which are plausible, with respect to the conceptual assumptions made.

6 REFERENCES

Bear J, Verruijt A, 1987. Modelling Groundwater Flow and Pollution. D. Reidel Publishing Company, Dordrecht, Holland.

Boulton G.S, Hulton N, Wallroth T, 1995. Impacts of long-term climate change on subsurface conditions: Time sequences, scenarios and boundary conditions for safety assessments. A report for Svensk Kärnbränslehantering AB.

Rhén I (ed), Gustafson G, Stanfors R, Wikberg P, 1997. Äspö HRL – Geoscientific evaluation 1997/5. Models based on site characterization 1986-1995. SKB Technical Report 97-06.

Spalding D.B, 1981. "A general purpose computer program for multi-dimensional one- and two-phase flow". Math. Comp. Sim., 8, 267-276. See also: http://www.cham.co.uk.

Svensson U, 1996. SKB Palaeohydrogeological programme. Regional groundwater flow due to an advancing and retreating glacier –scoping calculations. SKB Progress Report U-96-35.

Svensson U, 1996. SKB Palaeohydrogeological programme. Simulations of regional groundwater flows, as forced by glaciation cycles.. SKB Progress Report U-96-36.

Svensson U, 1997. A regional analysis of groundwater flow and salinity distribution in the Äspö area. SKB Technical Report 97-09.

APPENDIX A

DOCUMENTATION

CONDENSED DESCRIPTION OF GROUNDWATER FLOW MODEL.

Subglacial groundwater flow at Äspö as governed by basal melting and ice tunnels	
Scope: Groundwater and salinity distributions below a glacier	
Process description Conservation of mass, volume and momentum (Darcy´s law)	
CONCEPTS	**DATA**
Geometric framework and parameters	
Domain divided into computational cells to which conservation laws are applied. Subdomains consists of deterministic fracture zones and rock volumes between the fracture zones	Domain size: 250 x 10 x 4 m^3 Computational grid: 587 500 cells.
Material properties	
Hydraulic conductivities (K). Density varies with salinity. Transmissivity for fracture zones (T).	Data from Rhén et al (1997) and from calibration.
Spatial assignment method	
Fractures and fracture zones are represented in the computational grid. Small background conductivity added.	Data from Rhén et al (1997).
Boundary conditions	
Prescribed meltwater flux at ground level. Zero flux condition at all other boundaries.	Data from Boulton et al (1995).
Numerical tool PHOENICS	
Output parameters Flux, hydraulic head and salinity	